大 气 科 学 2005
Chinese Journal of Atmospheric Sciences
Volume 29, No.1, pp. 21–42

A Characteristic-Based Semi-Lagrangian Method for Hyperbolic Systems of Conservation Laws

Houjun Wang and *Gour-Tsyh Yeh*

(Department of Civil and Environmental Engineering, University of Central Florida, Orlando, Florida, USA)

Manuscript received 2 September 2004; revised 11 November 2004.

A characteristic-based semi-Lagrangian (CSL) method is developed for hyperbolic systems of conservation laws. In the CSL method, the governing equations are first transformed into a system of equations in characteristic form and then the Lagrangian form of the transformed equations is solved along the characteristic directions. By definition of hyperbolicity, such a transformation always exists. The CSL method is first illustrated by applying it to the one-dimensional (1-D) shallow water equations to solve the Rossby geostrophic adjustment problem. The authors then apply the CSL method to the 1-D fully-compressible, non-hydrostatic atmospheric equations to solve the hydrostatic adjustment problem. Transient solutions for both the linear and nonlinear problems are obtained and analyzed. It is shown that the CSL method produces more accurate solutions than the conventional semi-implicit semi-Lagrangian (SISL) method. It is also shown that the open boundary conditions can be easily implemented using the CSL method, which provides another advantage of the CSL method for regional atmospheric modeling. The extension to multi-dimensional hyperbolic systems is discussed and a simple demonstration is presented. The present study indicates that, although the SISL method is commonly used in the atmospheric models, the CSL method is potentially a better choice for fully-compressible, non-hydrostatic atmospheric modeling.

Key words: characteristic-based semi-Lagrangian method; hyperbolic systems; non-hydrostatic modeling; open boundary condition.

1 INTRODUCTION

A non-hydrostatic, fully-compressible atmospheric model is essentially hyperbolic in time. The eigenvalues are all real and wave motions are the main features of the system (Hirsch, 1988). For hyperbolic-dominant partial differential equations (PDEs), a characteristic-based semi-Lagrangian (CSL) method can be used. In the CSL method, the governing equations are first transformed into a system of equations in characteristic form and then one solves the Lagrangian form of the transformed equations along the characteristics. By definition, this transformation can always be done for a hyperbolic system. This method has its origin in the method of characteristics (MOC) in gas dynamics or free surface waves in hydraulic engineering. This is our first attempt to develop a semi-Lagrangian method based on the characteristic decomposition for non-hydrostatic atmospheric modeling.

The semi-Lagrangian method is widely used in meteorological modeling. However, in the conventional semi-Lagrangian method, only the prime characteristic directions, i.e., the directions associated with the local wind, are considered (Staniforth and Cote, 1991, p.2213). The CSL method is different from the conventional semi-implicit, semi-Lagrangian (SISL) method. In the SISL method, the acoustic mode is treated using an implicit scheme, while the Lagrangian method is used for other wave components where only wind is used for advection. In the CSL method, the PDEs are first transformed to their characteristic form. The transformed equations are solved using the Lagrangian method similar to that used in the SISL method, except that the characteristic velocities are used for advection.

The Rossby geostrophic adjustment and hydrostatic adjustment processes are two fundamental processes in the atmosphere. The fast-moving gravity waves and acoustic waves play an essential role in the two adjustment processes. A non-hydrostatic, fully-compressible atmospheric model permits both these types of waves and the associated adjustment processes. Therefore, numerical methods applied to this kind of model should treat these fast-moving gravity waves and acoustic waves accurately in order to accurately simulate the adjustment processes and related phenomena. The present study indicates that the CSL method can be such a method. Furthermore, the CSL method is also found well suited for the implementation of open boundary conditions.

The purposes of this paper are: (a) to develop the CSL method for hyperbolic systems of conservation laws and illustrate it in the 1-D systems; (b) to compare the CSL method with the conventional SISL method in solving the hydrostatic adjustment problem; and (c) to illustrate the implementation of the open boundary condition problem with the CSL method. The extension to the multi-dimensional problems is also discussed.

In the next section, the CSL method is illustrated in the 1-D shallow water systems to solve the Rossby adjustment problem. Section 3 applies the CSL method to the 1-D non-hydrostatic atmospheric model to solve the hydrostatic adjustment problem. Comparisons of the CSL method with the conventional SISL method are given in Section 4, followed by a discussion on open boundary conditions. Section 6 discusses the extension to the multi-dimensional hyperbolic systems. Summary and conclusions are given in Section 7. The details of the SISL method are given in the Appendix.

2 THE CSL METHOD FOR THE 1-D SHALLOW WATER MODEL

We first illustrate the CSL method by applying it to the 1-D shallow water equations to solve the Rossby adjustment problem. The 1-D inviscid, nonlinear shallow water equations can be written in the form:

$$\frac{\partial V}{\partial t} + A\frac{\partial V}{\partial x} = Q, \tag{2.1}$$

where

$$V = \begin{bmatrix} u \\ v \\ h \end{bmatrix}, \quad A = \begin{bmatrix} u & 0 & g \\ 0 & u & 0 \\ h & 0 & u \end{bmatrix}, \quad Q = \begin{bmatrix} +fv \\ -fu \\ 0 \end{bmatrix}.$$

The notation is standard: u and v are velocities in the x and y directions, h is the depth of fluid, g is the acceleration due to gravity, and f is the Coriolis parameter. In the CSL method, Eq. (2.1) is first transformed into the characteristic form through a diagonalization procedure in the following way:

1) Solve the eigenvalue equation

$$|\lambda I - A| = 0 \tag{2.2}$$

to get three real eigenvalues:

$$\lambda_1 = u, \quad \lambda_2 = u + c, \quad \lambda_3 = u - c, \tag{2.3}$$

where $c = \sqrt{gh}$. These eigenvalues are also called the characteristic velocities (Kulikovskii et al., 2001, p.3);

2) Compose the diagonalization matrix L^{-1} by the left eigenvectors, and the matrix L by the right eigenvectors in the column:

$$L^{-1} = \begin{bmatrix} 0 & 1 & 0 \\ 1 & 0 & +\frac{c}{h} \\ 1 & 0 & -\frac{c}{h} \end{bmatrix}, \quad L = \begin{bmatrix} 0 & \frac{1}{2} & \frac{1}{2} \\ 1 & 0 & 0 \\ 0 & \frac{h}{2c} & -\frac{h}{2c} \end{bmatrix}; \tag{2.4}$$

3) Define the characteristic variables δW as:

$$\delta W = L^{-1}\delta V = \begin{bmatrix} \delta v \\ \delta u + \frac{c}{h}\delta h \\ \delta u - \frac{c}{h}\delta h \end{bmatrix}; \tag{2.5}$$

4) The characteristic form equations become:

$$\frac{\partial W}{\partial t} + L^{-1}AL\frac{\partial W}{\partial x} = L^{-1}Q, \tag{2.6}$$

or

$$\frac{\partial W}{\partial t} + \begin{bmatrix} u & 0 & 0 \\ 0 & u+c & 0 \\ 0 & 0 & u-c \end{bmatrix} \frac{\partial W}{\partial x} = F, \tag{2.7}$$

where forcing terms F are given by

$$F = L^{-1}Q = \begin{bmatrix} F_1 \\ F_2 \\ F_3 \end{bmatrix} = \begin{bmatrix} -fu \\ +fv \\ +fv \end{bmatrix}.$$

We write Eq. (2.7) in the Lagrangian form as follows:

$$\frac{D_1 v}{Dt} = F_1, \tag{2.8}$$

$$\frac{D_2 u}{Dt} + \frac{c}{h}\frac{D_2 h}{Dt} = F_2, \tag{2.9}$$

$$\frac{D_3 u}{Dt} - \frac{c}{h}\frac{D_3 h}{Dt} = F_3, \tag{2.10}$$

where

$$\frac{D_1}{Dt} = \frac{\partial}{\partial t} + u\frac{\partial}{\partial x}, \quad \frac{D_2}{Dt} = \frac{\partial}{\partial t} + (u+c)\frac{\partial}{\partial x}, \quad \frac{D_3}{Dt} = \frac{\partial}{\partial t} + (u-c)\frac{\partial}{\partial x}.$$

Equations (2.8)–(2.10) are then solved along the three characteristics, respectively:

$$C_0 : dx/dt = u, \quad C_+ : dx/dt = u + c, \quad C_- : dx/dt = u - c.$$

Because the Lagrangian trajectories are calculated along the three characteristics using their respective characteristic wave velocities, we will call this procedure as the characteristic wave tracking.

The characteristics do not change except in the discontinuity (Courant and Hilbert, 1962, p.408). This underlying mathematical principle in the CSL method not only makes it both mathematically and physically sound, but also makes it more accurate than the conventional semi-Lagrangian method where only the fluid velocity is used for tracking. When the discontinuity appears, multiple solutions may exist near the discontinuity. This may pose some difficulties, especially in the multi-dimensional problems. In this case, entropy conditions could be invoked (Lax, 1973).

For the 1-D shallow water model, a more compact form of characteristic variables can be used (Erbes, 1993; Durran, 1999). However, we have chosen the present form to be consistent with the 1-D non-hydrostatic atmospheric model and to readily extend it to the multi-dimensional problems. It should also be noted that relevant discussion on the method of characteristics for the 1-D systems can be found in Gustafsson et al. (1995, p.309–310).

The two-time-level scheme is used for the temporal discretization to avoid the well-known computational mode in the three-time-level scheme. The simple Picard iteration method is chosen in the solution. Only a few (< 5) iterations are necessary to achieve accurate results. No time filter is used because there is no computational mode for the two-time-level scheme. The simple linear interpolation method is used for both spatial or temporal interpolations. Other integration schemes, such as a 4th-order Runge-Kutta (RK4) scheme, could also be used. Small and sub-cycling time-steps could also be used for the fast-moving characteristic waves if necessary.

The prototype Rossby adjustment problem studies the time evolution of an initially motionless fluid layer with a discontinuity in the height field. The initial conditions are (Gill, 1982, p.192):

$$u(x,0) = v(x,0) = 0$$
$$h(x,0) = H - \eta_0 \ \mathrm{sgn}(x)$$

where the $\mathrm{sgn}(x)$ is the sign function (sign of x) defined by

$$\mathrm{sgn}(x) = \begin{cases} 1, & \text{for } x > 0, \\ -1, & \text{for } x < 0, \end{cases}$$

and the other parameters are: $\bar{c} = \sqrt{gH}$ =10 m s^{-1}, $f = 10^{-4}$ s^{-1}. The so-called Rossby radius of deformation is given by $a = \bar{c}/|f|$ =10 m s^{-1}/10^{-4} s^{-1} = 10^5 m=100 km. The analytical solution for the linear problem is given in Gill (1982, p.198–201). The numerical solutions of the nonlinear geostrophic adjustment problem can be found in Kuo and Povani (1997), where a more sophisticated numerical package is used.

A uniform grid with grid size $\Delta x = 10^3$ m was used, and the time step is $\Delta t = 4\Delta x/\bar{c}$. This time step was chosen so that the damping due to the linear interpolation can be reduced/eliminated for the linear problem. For more complicated problems of general applications, other shape-preserving or monotonic interpolation schemes, such as those of Williamson and Rasch (1989), could be used.

The CSL solutions of the Rossby adjustment problem are shown in Figs. 1–3, where $\eta = h - H$. The solutions are shown at time intervals of $50\Delta t$, where Δt is the time step;

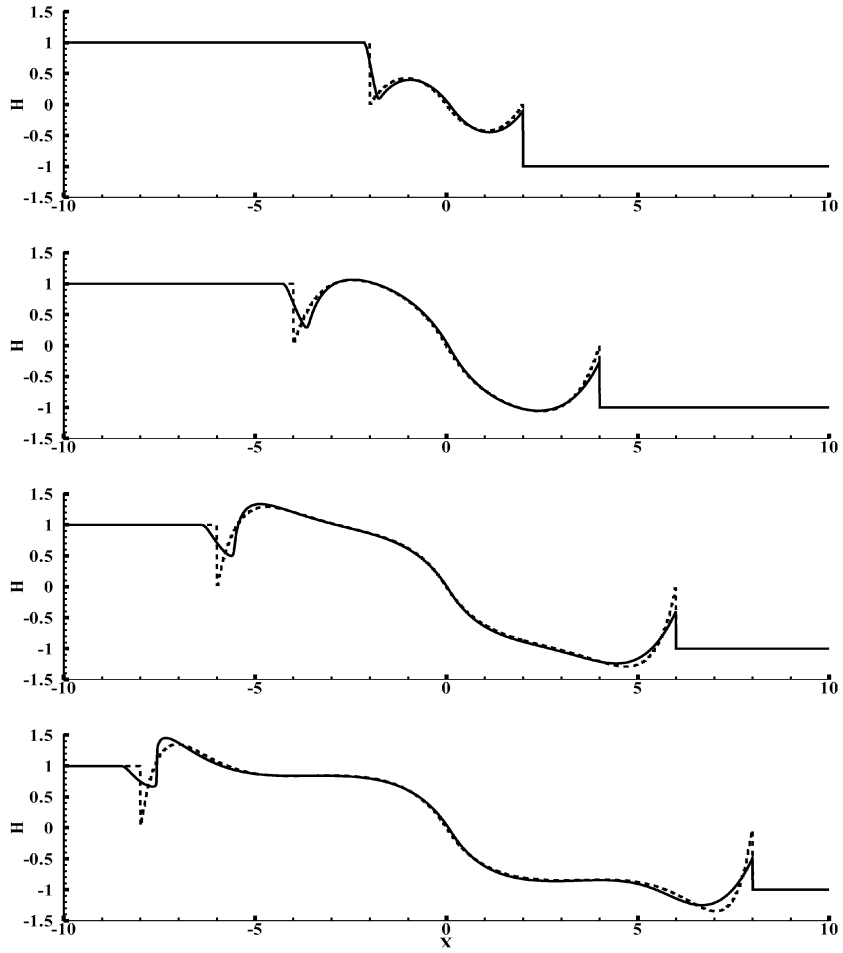

Fig. 1: The CSL solutions of the Rossby adjustment problem: η/η_0 at time intervals of $2f^{-1}$. The solid curves are for the nonlinear problem, and the dashed curves are for the linear problem.

or $2f^{-1}$, where f is the Coriolis parameter. The solid curves are for the nonlinear problem, and the dashed curves are for the linear problem. The x-coordinate is scaled by the Rossby radius of deformation a, while η is scaled by η_0, and u and v are scaled by $(\eta_0/H)\bar{c}$. For the linear calculations, the solutions are almost indistinguishable from the analytical solutions. The nonlinear effects, e.g., advection by u, are also clearly captured by the CSL method. Thus, accurate solutions were obtained with little effort using the CSL method.

3 THE CSL METHOD FOR THE 1-D NON-HYDROSTATIC ATMOSPHERIC MODEL

The CSL method outlined in the previous section is now applied to the 1-D non-hydrostatic atmospheric model to solve the hydrostatic adjustment problem. The model is a fully-compressible, non-hydrostatic atmospheric model. With a heating source in the

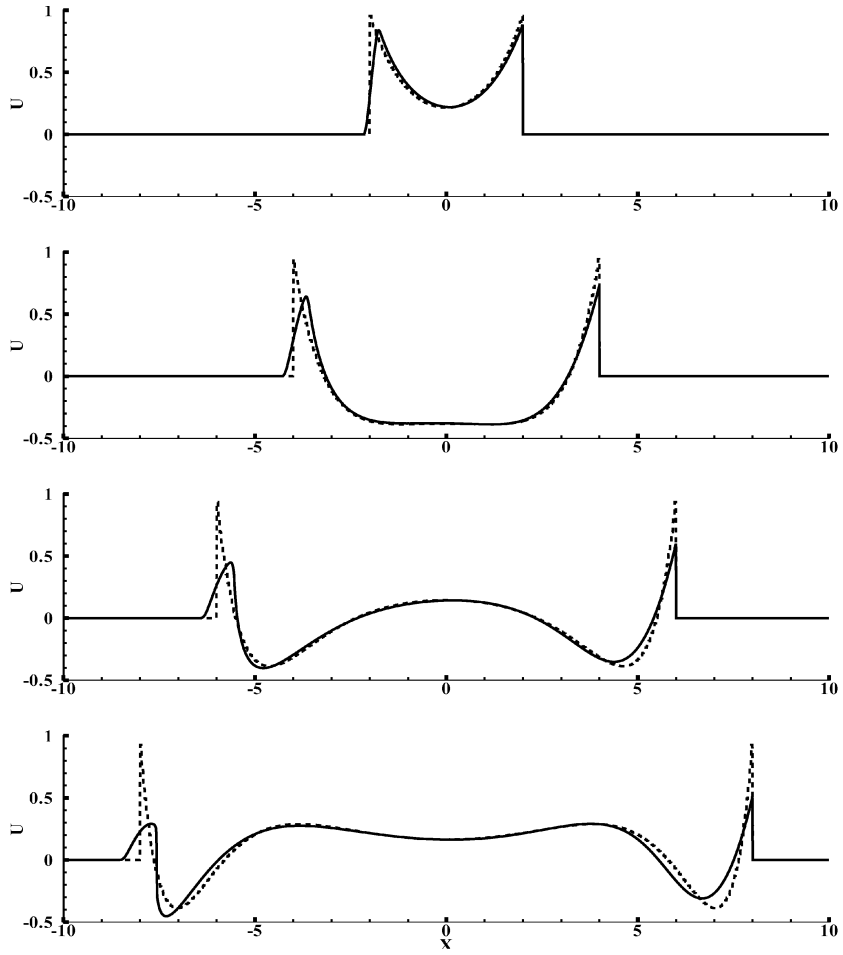

Fig. 2: The CSL solutions of the Rossby adjustment problem: $u/[(\eta_0/H)\bar{c}]$ at time intervals of $2f^{-1}$. The solid curves are for the nonlinear problem, and the dashed curves are for the linear problem.

vertical column, the 1-D non-hydrostatic atmospheric model equations can be written as

$$\frac{\partial V}{\partial t} + C\frac{\partial V}{\partial z} = Q, \tag{3.1}$$

where

$$V = \begin{bmatrix} \rho \\ w \\ \Theta \end{bmatrix}, \quad C = \begin{bmatrix} w & \rho & 0 \\ 0 & w & \dfrac{\gamma R\pi}{\rho} \\ 0 & \Theta & w \end{bmatrix}, \quad Q = \begin{bmatrix} 0 \\ -g \\ \rho\dot{Q} \end{bmatrix}.$$

The notation is standard: w is the vertical velocity, ρ is the air density, $\Theta = \rho\theta$, θ is the potential temperature, π is the Exner function defined as $\pi = (p/p_0)^{\kappa}$, $\kappa = R/c_p$, and $\gamma = c_p/c_v = 1.4$ is the ratio of the heat capacities for dry air. $\dot{Q}$ is the heating function, where one form is given in (3.6). Using the procedures outlined in the previous section, we obtain the it characteristic form equations of (3.1) as follows:

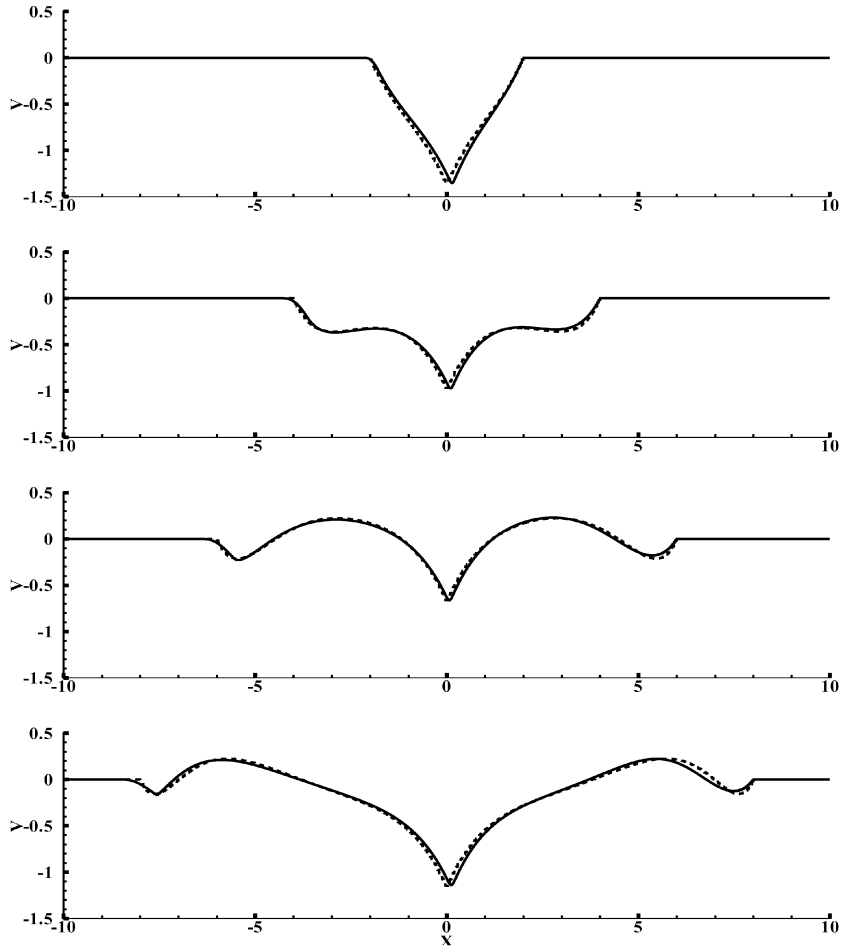

Fig. 3: The CSL solutions of the Rossby adjustment problem: $v/[(\eta_0/H)\bar{c}]$ at time intervals of $2f^{-1}$. The solid curves are for the nonlinear problem, and the dashed curves are for the linear problem.

$$\frac{\partial W}{\partial t} + \begin{bmatrix} w & 0 & 0 \\ 0 & w+c & 0 \\ 0 & 0 & w-c \end{bmatrix} \frac{\partial W}{\partial z} = F, \tag{3.2}$$

where $c = \sqrt{\frac{\gamma R\pi}{\rho}\Theta}$ is the speed of sound, and the characteristic variables δW and the forcing terms F are

$$\delta W = \begin{bmatrix} \delta\rho - \dfrac{\gamma R\pi}{c^2}\delta\Theta \\ \delta w + \dfrac{\gamma R\pi}{\rho c}\delta\Theta \\ \delta w - \dfrac{\gamma R\pi}{\rho c}\delta\Theta \end{bmatrix}, \quad F = \begin{bmatrix} F_1 \\ F_2 \\ F_3 \end{bmatrix} = \begin{bmatrix} -\rho\dot{Q}\left(\dfrac{\gamma R\pi}{c^2}\right) \\ -g + \rho\dot{Q}\left(\dfrac{\gamma R\pi}{\rho c}\right) \\ -g - \rho\dot{Q}\left(\dfrac{\gamma R\pi}{\rho c}\right) \end{bmatrix}.$$

The Lagrangian form of (3.1) is

$$\frac{D_1\rho}{Dt} - \frac{\rho}{\Theta}\frac{D_1\Theta}{Dt} = F_1, \tag{3.3}$$

$$\frac{D_2 w}{Dt} + \frac{c}{\Theta}\frac{D_2\Theta}{Dt} = F_2, \tag{3.4}$$

$$\frac{D_3 w}{Dt} - \frac{c}{\Theta}\frac{D_3\Theta}{Dt} = F_3, \tag{3.5}$$

where

$$\frac{D_1}{Dt} = \frac{\partial}{\partial t} + w\frac{\partial}{\partial z}, \quad \frac{D_2}{Dt} = \frac{\partial}{\partial t} + (w+c)\frac{\partial}{\partial z}, \quad \frac{D_3}{Dt} = \frac{\partial}{\partial t} + (w-c)\frac{\partial}{\partial z}.$$

Equations (3.3)–(3.5) are solved along the three characteristics, respectively:

$$C_0 : dz/dt = w, \quad C_+ : dz/dt = w + c, \quad C_- : dz/dt = w - c.$$

Therefore, in the CSL method, the acoustic waves are treated explicitly, the same as for the other waves. The Lagrangian time-difference operator of (A10) is used for the total time derivatives, and the trajectory-average operator of (A12) is used for the coefficients and the right hand side forcing terms. Note that deviations ρ' and Θ' from a time invariant, hydrostatically balanced reference state $\bar{\rho}(z)$ and $\bar{\Theta}(z)$ can be defined such that $\rho = \bar{\rho}(z) + \rho'$ and $\Theta = \bar{\Theta}(z) + \Theta'$, and Eqs. (3.3)–(3.5) can then be solved for ρ' and Θ'. No approximation is introduced in this procedure.

The prototype hydrostatic adjustment problem considers the response of a horizontally homogeneous, initially hydrostatic, isothermal atmosphere to an instantaneous heating in the middle of the atmosphere column. The heating function has the following form (Bannon, 1995):

$$\dot{Q} = \frac{\theta_0}{\rho_0 c_p T_0} Q_h, \tag{3.6}$$

where

$$Q_h = \frac{c_v}{R}\Delta p[H(z+a) - H(z-a)]\delta(t)$$

is the heating per unit volume. H is the Heaviside step function and $\delta(t)$ is the Dirac delta function. $\delta(t)$ has a dimension of t^{-1}, and in the temporal discretization, it is replaced by $1/\Delta t$, where Δt is the time step. The analytical solutions of the linear problem can be found in Bannon (1995) and Sotack and Bannon (1990).

The CSL solutions of the linear hydrostatic adjustment problem are shown in Figs. 4–6. The CSL solutions of the nonlinear hydrostatic adjustment problem are shown in Figs. 7–9. In these calculations, uniform grids with grid size $\Delta z = 200$ m were used. The time step is $\Delta t = \Delta z/\bar{c}_s$, although a larger time step could be used without causing any computational instability.

All results are for Δp=100 Pa, unless otherwise stated. The results w, ρ', and θ' are scaled by $\Delta w = \Delta p/(2\rho_* \bar{c}_s)$, $\Delta\rho = \Delta p/(gH_s)$, and $\Delta\theta = T_0\Delta p/p_*$, respectively. The subscript * denotes a constant reference value, and $\bar{c}_s = (\gamma R T_0)^{1/2}$ is the speed of sound and $T_0 = 267$. The units of the z-coordinate are in km. Figure 4 also compares the CSL solution (solid curves) and the analytical solutions (dashed curves; Eq. (3.5) in Bannon, 1995). The effects of nonlinearity are shown by comparing solutions with $\Delta p = 100$ Pa and Δp= 1000 Pa in Figs. 7–9.

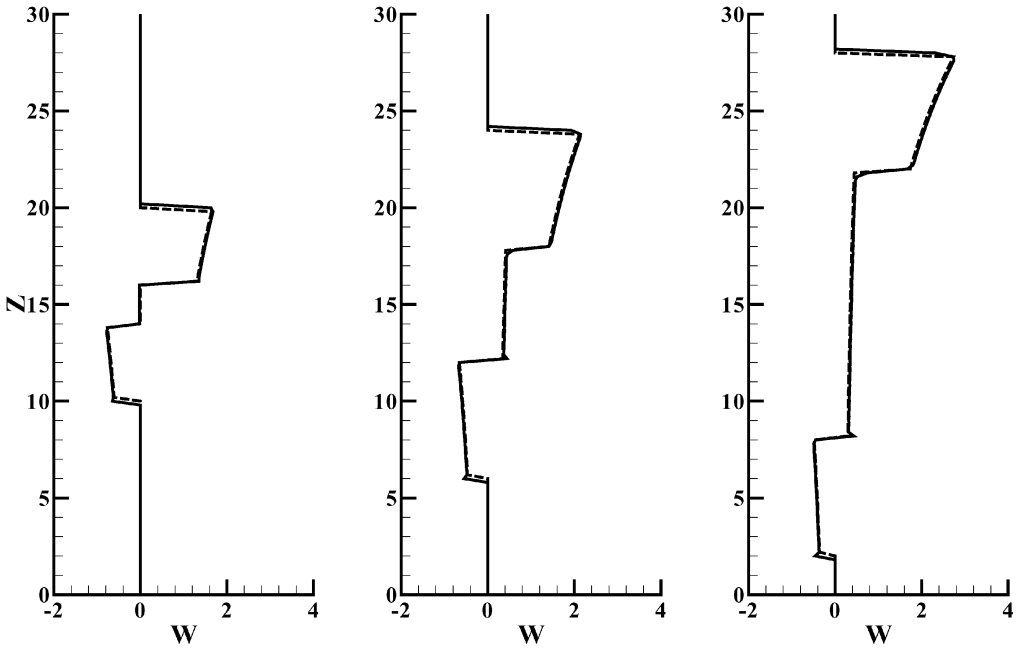

Fig. 4: The CSL and analytical solutions of the linear hydrostatic adjustment problem: $w/\Delta w$ at time steps 10, 30, and 50. The solid curves are for the CSL solutions, the dashed curves are for the analytical solutions.

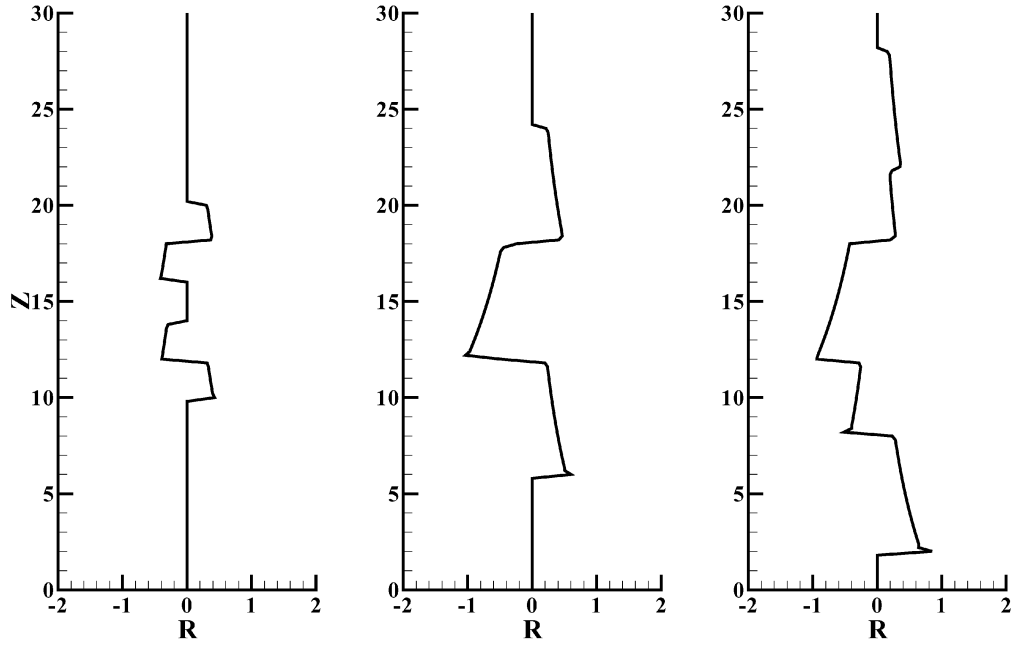

Fig. 5: The CSL solutions of the linear hydrostatic adjustment problem: $\rho'/\Delta\rho$ at time steps 10, 30, and 50.

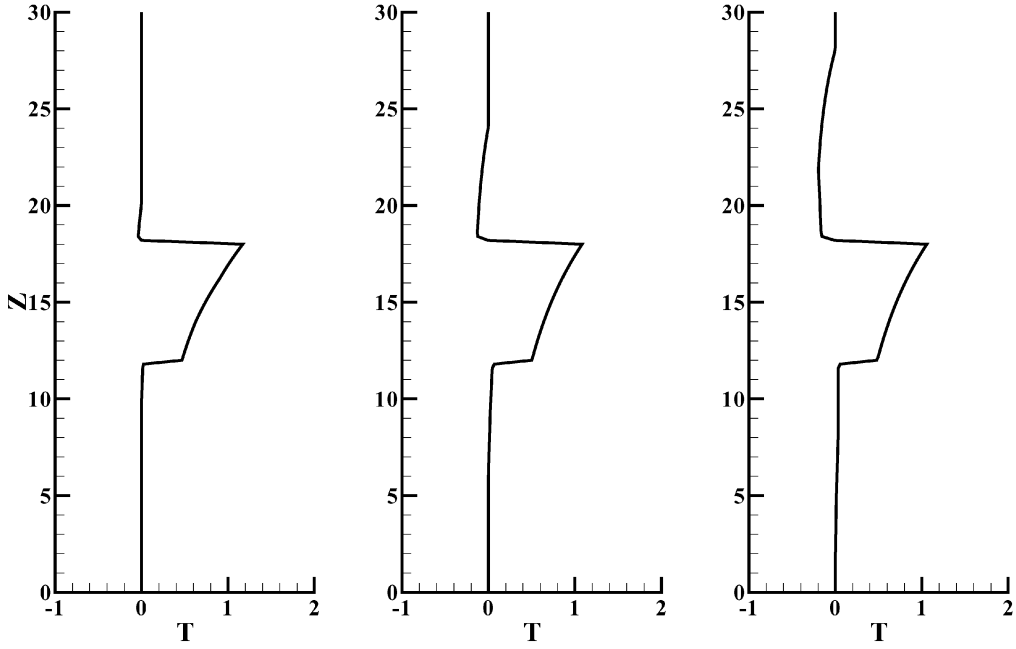

Fig. 6: The CSL solutions of the linear hydrostatic adjustment problem: $\theta'/\Delta\theta$ at time steps 10, 30, and 50.

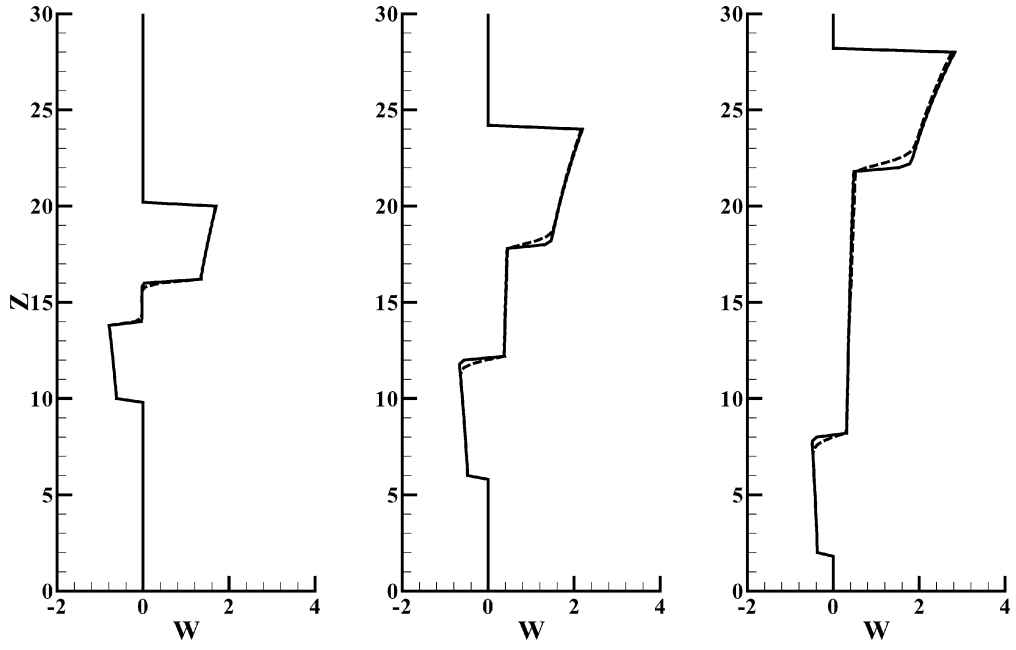

Fig. 7: The CSL solutions of the nonlinear hydrostatic adjustment problem: $w/\Delta w$ at time steps 10, 30, and 50. The solid curves are for case $\Delta p = 100$, and the dashed curves are for case $\Delta p = 1000$.

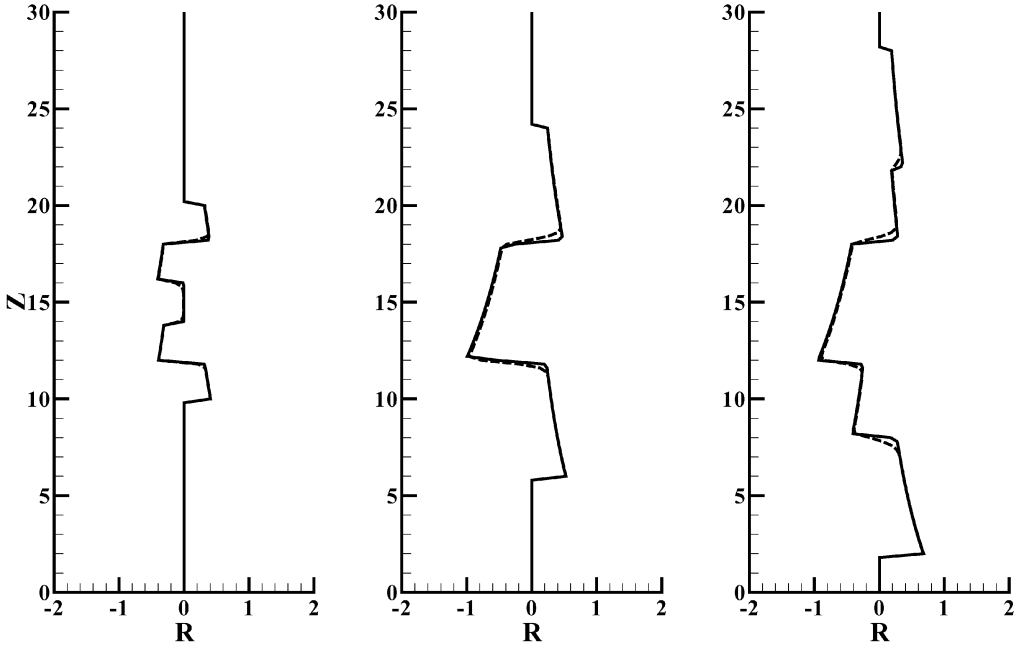

Fig. 8: The CSL solutions of the nonlinear hydrostatic adjustment problem: $\rho'/\Delta\rho$ at time steps 10, 30, and 50. The solid curves are for case $\Delta p = 100$, and the dashed curves are for case $\Delta p = 1000$.

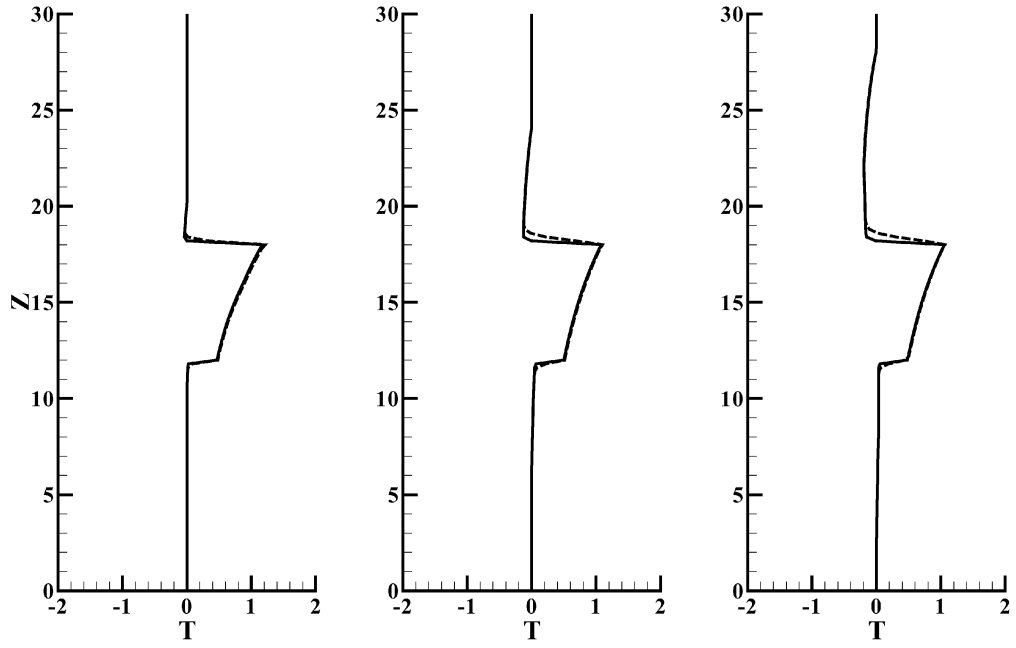

Fig. 9: The CSL solutions of the nonlinear hydrostatic adjustment problem: $\theta'/\Delta\theta$ at time steps 10, 30, and 50. The solid curves are for case $\Delta p = 100$, and the dashed curves are for case $\Delta p = 1000$.

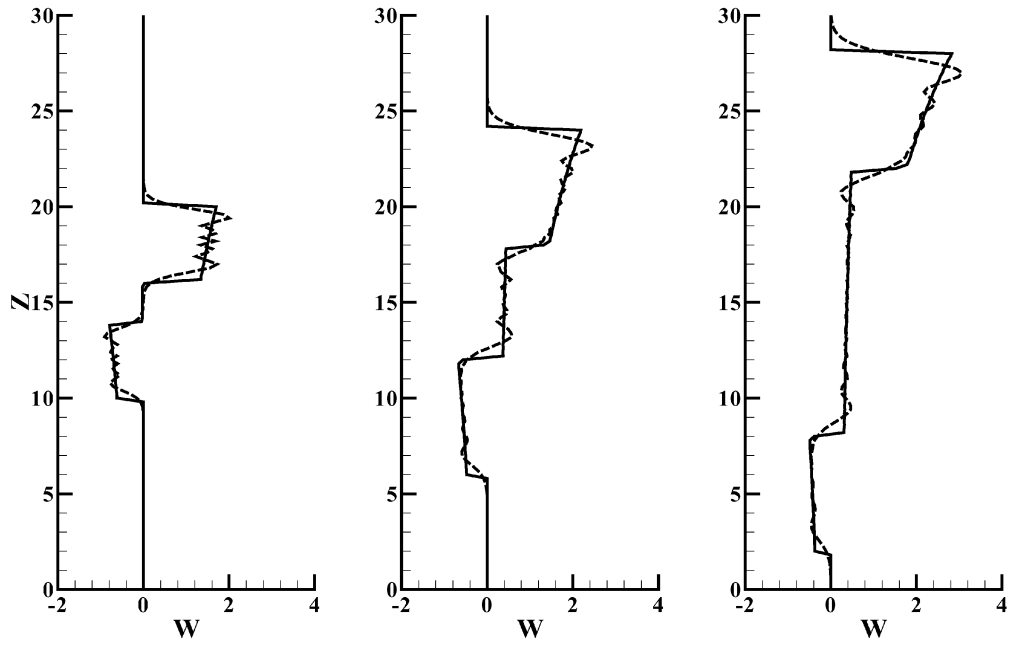

Fig. 10: The CSL and SISL solutions of the nonlinear hydrostatic adjustment problem: $w/\Delta w$ at time steps 10, 30, and 50. The solid curves are for the CSL solutions, and the dashed curves are for the SISL solutions.

4 COMPARISON WITH THE SISL METHOD

In this section, the CSL method is compared with the SISL method. The details of the SISL method are given in the Appendix. Unlike the CSL method, the SISL method treats the acoustic waves implicitly to ensure that a large time step can be used, and it uses only wind for the Lagrangian tracking. In the calculations presented below, fixed upper and lower boundary conditions are used.

Figures 10–12 compare the CSL and SISL solutions of the nonlinear hydrostatic adjustment problem. The improvements of the CSL solutions over the SISL solutions are that the CSL method can handle problems with sharp gradients easily and can obtain accurate solutions with less numerical oscillations efficiently. Note that this improvement is not due to the different upper or lower boundary conditions used in the solutions, because the solutions are not influenced by the boundary conditions yet.

5 OPEN BOUNDARY CONDITIONS

When the equations are written in the characteristic form, it is convenient to implement the so-called open boundary conditions. In the present case, the flows are subcritical ($u < c$) or subsonic ($w < c_s$). Only one boundary condition is needed at each boundary, that is, when the backward characteristic wave tracking is started from the boundary within each time step. In such a case, the value at the boundary can be approximated by interpolation from the value at time t and the value at time $t + \Delta t$ (from the previous iteration). This is the only approximation, and it is consistent with the idea that there is no flux of information into the domain of computation. The numerical results indicate this simple scheme for open boundary conditions is an appropriate implementation.

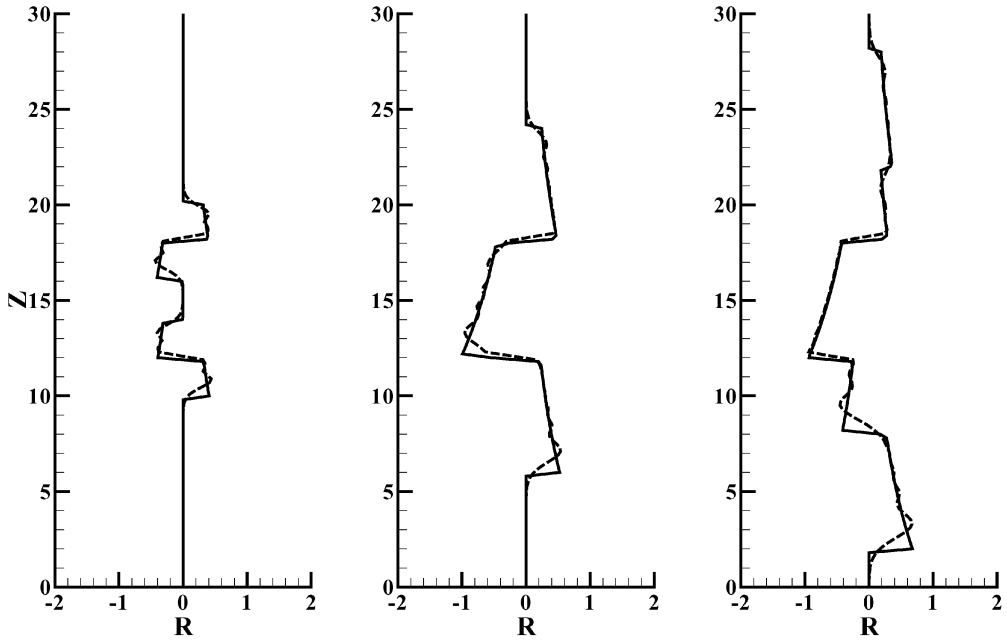

Fig. 11: The CSL and SISL solutions of the nonlinear hydrostatic adjustment problem: $\rho'/\Delta\rho$ at time steps 10, 30, and 50. The solid curves are for the CSL solutions, and the dashed curves are for the SISL solutions.

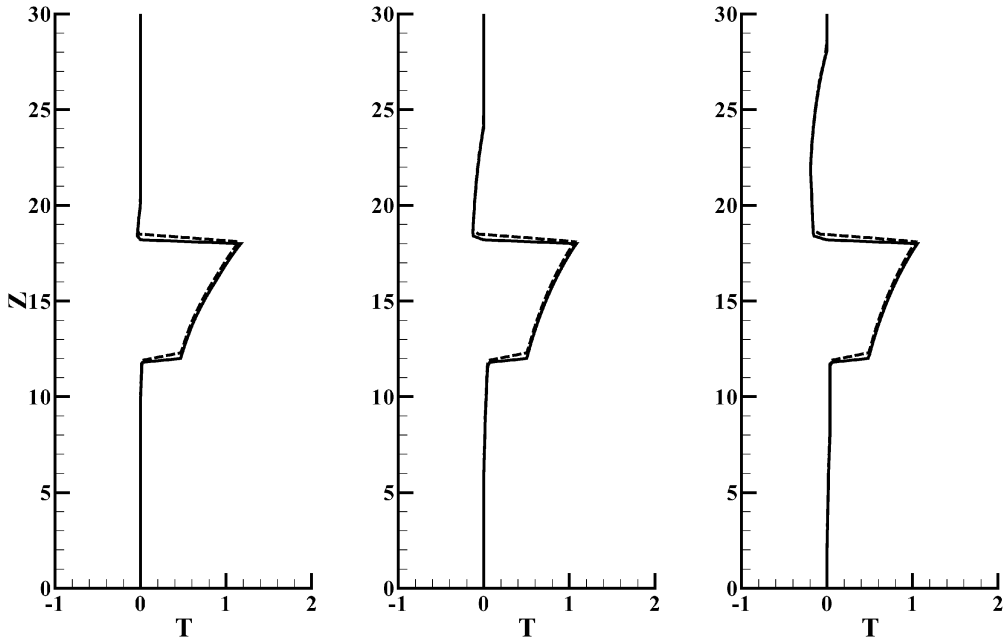

Fig. 12: The CSL and SISL solutions of the nonlinear hydrostatic adjustment problem: $\theta'/\Delta\theta$ at time steps 10, 30, and 50. The solid curves for the CSL solutions, and the dashed curves for the SISL solutions.

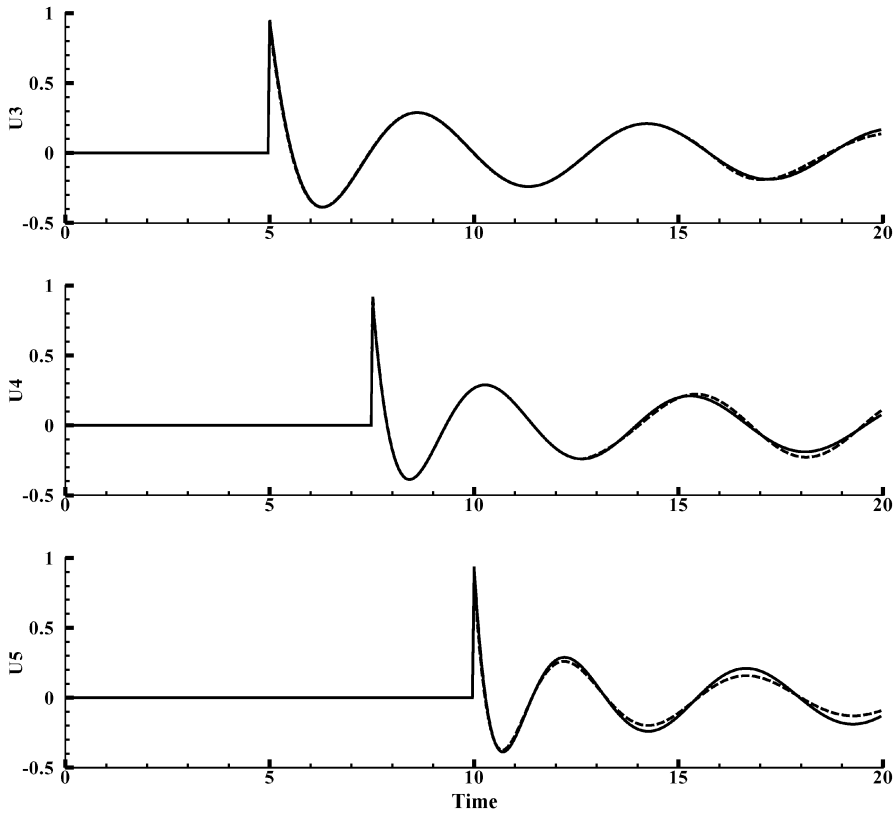

Fig. 13: The CSL and analytical solutions of the linear Rossby adjustment problem: $u/[(\eta_0/H)\bar{c}]$. The solid curves are for the analytical solutions, and the dashed curves are for the CSL solutions. U5 is the the right boundary, and U4 and U3 are $1/8L$ and $1/4L$ away from the right boundary, respectively, where L is the total length of the computational domain. The time is scaled by the Coriolis parameter f.

Figure 13 compares the results of the CSL method and the analytical solution of the 1-D linear Rossby adjustment problem. It shows that the numerical solution is very close to the analytical solutions. In the interior points, the numerical solutions are almost indistinguishable from the analytical solutions. Figure 14 compares the CSL solutions with the analytical solutions of the linear hydrostatic adjustment problem.

The open boundary conditions implemented in this study belong to the so-called 'perfectly non-reflecting boundary conditions' category. The partially non-reflecting boundary conditions similar to Poinsot and Lele (1992) show no improvement in the solutions, or even make them worse sometimes, and will not be shown here.

With fixed boundary conditions in the SISL method, the solutions can be contaminated quickly by the reflecting boundary waves. The open boundary conditions may also be implemented similarly in the SISL method. However, this implementation cannot solve all the problems in this case because the acoustic waves are not treated explicitly. That is, we still need to implement open boundary conditions in solving the elliptic equation (A21) for the acoustic modes. Durran (2001) gives an interesting discussion on open boundary conditions.

The easy and physically-sound implementation of the open boundary conditions make the

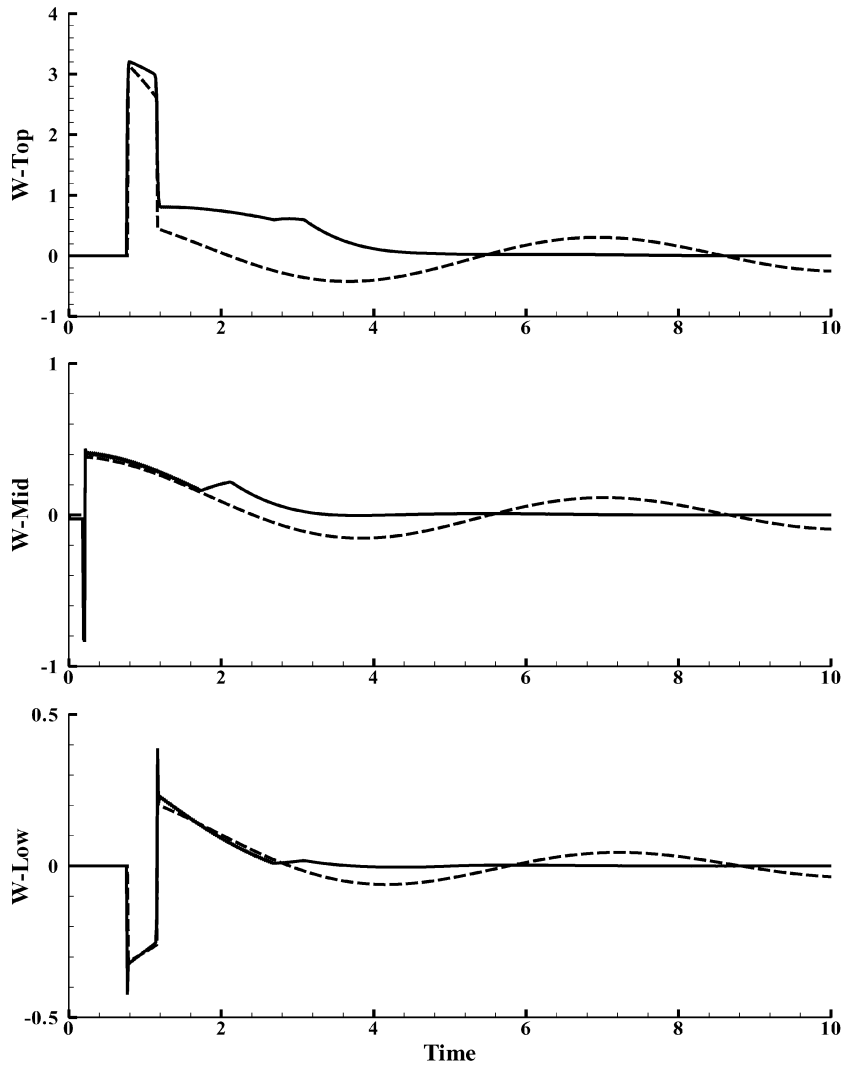

Fig. 14: The CSL and analytical solutions of the linear hydrostatic adjustment problem: $w/\Delta w$. The solid curves are for the CSL solutions, and the dashed curves are for the analytical solutions. The time is scaled by the acoustic cutoff frequency $N_a = \bar{c}_s/(2H_s)$, where $\bar{c}_s$ is the speed of sound and $H_s = RT_0/g$ is the scale height.

CSL method more advantageous over the conventional semi-Lagrangian methods, both for regional atmospheric modeling and for global atmospheric modeling where open boundary conditions may be used at the top of the model. This implementation is a better choice than the artificial diffusive boundary conditions that are usually used in the atmospheric models.

6 EXTENSION TO THE MULTI-DIMENSIONAL PROBLEMS

In this section, the extension of the CSL method to the multi-dimensional problems is discussed. Although in the 1-D case only left or right characteristic directions exist, in the multi-dimensional cases there are an infinite number of characteristic directions that could

be used for the characteristic wave tracking. The best choice is to choose the characteristic directions that can minimize the coupled terms. This is illustrated with the 2-D shallow water equations.

The 2-D inviscid, nonlinear shallow water model equations can be written in the form:

$$\frac{\partial V}{\partial t} + A\frac{\partial V}{\partial x} + B\frac{\partial V}{\partial y} = Q, \tag{6.1}$$

where

$$V = \begin{bmatrix} u \\ v \\ h \end{bmatrix}, \quad A = \begin{bmatrix} u & 0 & g \\ 0 & u & 0 \\ h & 0 & u \end{bmatrix}, \quad B = \begin{bmatrix} v & 0 & 0 \\ 0 & u & g \\ 0 & h & v \end{bmatrix}, \quad Q = \begin{bmatrix} +fv \\ -fu \\ 0 \end{bmatrix}.$$

The notation is standard. As in the 1-D case, the CSL method first transforms Eq. (6.1) into its characteristic form through a diagonalization procedure in the following way:

1) Solve the eigenvalue equation

$$|\lambda I - (Ak_x + Bk_y)| = 0 \tag{6.2}$$

to get three real eigenvalues, which, by definition of hyperbolicity, always exist (e.g., Kulikovskii et al., 2001, p.2):

$$\lambda_1 = uk_x + vk_y, \quad \lambda_2 = uk_x + vk_y + c, \quad \lambda_3 = uk_x + vk_y - c, \tag{6.3}$$

where $c = \sqrt{gh}$, and k_x and k_y are the Cartesian components of the unit vector $\boldsymbol{k}$;

2) Compose the diagonalization matrix L^{-1} by the left eigenvectors:

$$L^{-1} = \begin{bmatrix} k_y & -k_x & 0 \\ k_x & k_y & +\dfrac{c}{h} \\ k_x & 0 & -\dfrac{c}{h} \end{bmatrix}, \tag{6.4}$$

and the matrix L by the right eigenvectors in the column:

$$L = \begin{bmatrix} k_y & \dfrac{k_x}{2} & \dfrac{k_y}{2} \\ -k_x & \dfrac{k_y}{2} & \dfrac{k_x}{2} \\ 0 & \dfrac{h}{2c} & -\dfrac{h}{2c} \end{bmatrix}; \tag{6.5}$$

3) Define the characteristic variables δW as:

$$\delta W = L^{-1}\delta V = \begin{bmatrix} k_y\delta u - k_x\delta v \\ k_x\delta u + k_y\delta v + \dfrac{c}{h}\delta h \\ k_x\delta u + k_y\delta v - \dfrac{c}{h}\delta h \end{bmatrix}; \tag{6.6}$$

4) The characteristic form equations become:

$$\frac{\partial W}{\partial t} + L^{-1}AL\frac{\partial W}{\partial x} + L^{-1}BL\frac{\partial W}{\partial y} = L^{-1}Q, \tag{6.7}$$

or

$$\frac{\partial W}{\partial t}+\begin{bmatrix}u & 0 & 0\\ 0 & u+ck_x & 0\\ 0 & 0 & u-ck_x\end{bmatrix}\frac{\partial W}{\partial x}+\begin{bmatrix}v & 0 & 0\\ 0 & v+ck_y & 0\\ 0 & 0 & v-ck_y\end{bmatrix}\frac{\partial W}{\partial y}+S=F, \tag{6.8}$$

where the coupled terms, S, are given by

$$S=\begin{bmatrix}S_1\\ S_2\\ S_3\end{bmatrix}=\begin{bmatrix}g(k_y\dfrac{\partial h}{\partial x}-k_x\dfrac{\partial h}{\partial y})\\ +c[k_yk_y\dfrac{\partial u}{\partial x}-k_xk_y(\dfrac{\partial v}{\partial x}+\dfrac{\partial u}{\partial y})+k_xk_x\dfrac{\partial v}{\partial y}]\\ -c[k_yk_y\dfrac{\partial u}{\partial x}-k_xk_y(\dfrac{\partial v}{\partial x}+\dfrac{\partial u}{\partial y})+k_xk_x\dfrac{\partial v}{\partial y}]\end{bmatrix}, \tag{6.9}$$

and the forcing terms F are given by:

$$F=L^{-1}Q=\begin{bmatrix}F_1\\ F_2\\ F_3\end{bmatrix}=\begin{bmatrix}k_yfv-k_xfu\\ k_xfv-k_yfu\\ k_xfv-k_yfu\end{bmatrix}. \tag{6.10}$$

We write Eq. (6.8) in the Lagrangian form as follows:

$$k_y\frac{D_1u}{Dt}-k_x\frac{D_1v}{Dt}=F_1-S_1, \tag{6.11}$$

$$k_x\frac{D_2u}{Dt}+k_y\frac{D_2v}{Dt}+\frac{c}{h}\frac{D_2h}{Dt}=F_2-S_2, \tag{6.12}$$

$$k_x\frac{D_3u}{Dt}+k_y\frac{D_3u}{Dt}-\frac{c}{h}\frac{D_3h}{Dt}=F_3-S_3, \tag{6.13}$$

where

$$\frac{D_1}{Dt}=\frac{\partial}{\partial t}+u\frac{\partial}{\partial x}+v\frac{\partial}{\partial y},$$
$$\frac{D_2}{Dt}=\frac{\partial}{\partial t}+(u+ck_x)\frac{\partial}{\partial x}+(v+ck_y)\frac{\partial}{\partial y},$$
$$\frac{D_3}{Dt}=\frac{\partial}{\partial t}+(u-ck_x)\frac{\partial}{\partial x}+(u-ck_y)\frac{\partial}{\partial y}.$$

Equations (6.11)–(6.13) are the solved along the three characteristic curves, respectively:

$$C_0: dx/dt=u,\quad dy/dt=v;$$
$$C_+: dx/dt=u+ck_x,\quad dy/dt=v+ck_y;$$
$$C_-: dx/dt=u-ck_x,\quad dy/dt=v-ck_y.$$

As noted earlier, there are an infinite number of characteristic directions, $\boldsymbol{k}=(k_x,k_y)$, that could be used for the characteristic wave tracking. The optimal local characteristic directions can be so chosen that the coupled terms, S_1, S_2 and S_3, can vanish or be minimized and that a locally decoupled or nearly-decoupled system can be obtained. Deconinck et al. (1986) presented a procedure on how the decoupling can be done or how the S-terms can be minimized. A general minimization algorithm determining the optimal $\boldsymbol{k}$ directions will be developed and reported on a subsequent paper. Discussion on the characteristic form of the multi-dimensional Euler equations can also be found in Hirsch (1990, Chapter 16).

The above 2-D CSL method is demonstrated to solve the idealized circular dam-break problem (e.g., Toro, 2001). Assume a circular dam of radius R =5.0 m centered in a square computational domain of 40 m×40 m. The initial velocity fields are $u(x, y, 0) = v(x, y, 0) = 0$, and the initial water depth is

$$h(x, y, 0) = \begin{cases} h_{\text{ins}} = 1.0 \text{ m}, & \text{if } (x - x_c)^2 + (y - y_c)^2 \leqslant R^2, \\ h_{\text{out}} = 0.5 \text{ m}, & \text{if } (x - x_c)^2 + (y - y_c)^2 > R^2, \end{cases}$$

where (x_c, y_c) is the center of the circular dam. Both sharp gradients and shock waves exist in this problem.

For axisymmetric flow as in the idealized circular dam-break problem, the governing equations can also be written in the 1-D form in the radial direction r:

$$\frac{\partial u}{\partial t} + u\frac{\partial u}{\partial r} + g\frac{\partial h}{\partial r} = 0, \tag{6.14}$$

$$\frac{\partial h}{\partial t} + u\frac{\partial h}{\partial r} + h\frac{\partial u}{\partial r} = -\frac{hu}{r}. \tag{6.15}$$

In the CSL method, the above equations are written in the characteristic form:

$$\frac{D_2 u}{Dt} + \frac{c}{h}\frac{D_2 h}{Dt} = -\frac{cu}{r}, \tag{6.16}$$

$$\frac{D_3 u}{Dt} - \frac{c}{h}\frac{D_3 h}{Dt} = +\frac{cu}{r}, \tag{6.17}$$

where u is the radial velocity, and

$$\frac{D_2}{Dt} = \frac{\partial}{\partial t} + (u + c)\frac{\partial}{\partial r}, \quad \frac{D_3}{Dt} = \frac{\partial}{\partial t} + (u - c)\frac{\partial}{\partial r}.$$

Equations (6.16)–(6.17) are then solved along the two characteristics, respectively:

$$C_+ : dr/dt = u + c, \quad C_- : dr/dt = u - c.$$

To compare the 1-D and 2-D solutions, 1000 grid points were used for the 1-D solutions, and 200 × 200 grid points were used for the 2-D solutions. The time steps are 0.01 and 0.02 seconds, respectively. Figure 15 compares the 1-D and 2-D solutions of h and u at 0.7 s. The 1-D solution may be regarded as the exact solution. The 2-D solution is essentially axisymmetric, so only the slice crossing the first and third quadrants is used for comparison. The 2-D CSL solution captures the wave amplitude and speed fairly well. The numerical results also show that the CSL implementation of the open boundary conditions extends naturally to the 2-D problem.

The 2-D solutions shown in Fig. 15 were obtained by specifying the characteristic directions $\boldsymbol{k}$ in the outward radial directions. A general algorithm minimizing the S-terms will be developed and numerical results from multi-dimensional non-hydrostatic modeling will be reported subsequently.

7 SUMMARY AND CONCLUSIONS

We have illustrated the basic principle of a characteristic-based semi-Lagrangian (CSL) method and the basic procedures of implementation. We have implemented the CSL method to the 1-D shallow water model to solve the Rossby adjustment problem and the 1-D non-hydrostatic atmospheric model to solve the hydrostatic adjustment problem. Transient solutions for both linear and nonlinear problems are obtained and analyzed.

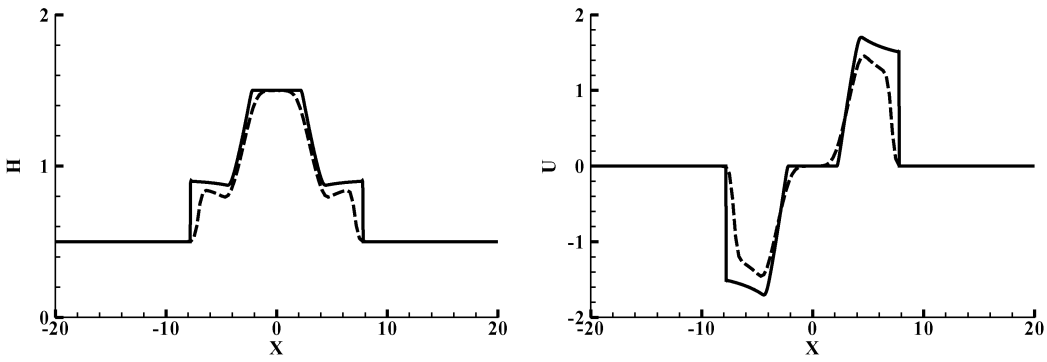

Fig. 15: Comparison of the 1-D and 2-D solutions for the idealized circular dam-break problem: h and u at time 0.7 s. The solid curves are for the high-resolution 1-D solution, and the dashed curves are for the 2-D solution.

It has been shown that the CSL method can better handle problems with a sharp gradient. Compared to the SISL method, accurate solutions with less numerical oscillations can be efficiently obtained with the CSL method. Open boundary conditions can also be readily implemented in the CSL method. Although it is also possible to implement a similar open boundary condition setup in the semi-implicit scheme, the CSL method provides a consistent approach to the solutions of open boundary problems.

Furthermore, errors in the observations could induce an imbalance in the initial conditions for atmospheric models. The initialization procedure is usually used to remove the unrealistic imbalance. We can expect that, by handling the fast-moving gravity waves and acoustic waves more accurately, the CSL method could produce more realistic geostrophic and hydrostatic adjustment in the models.

This study indicates that, although the SISL method may be preferred for solutions of the incompressible hydrostatic atmospheric equations, the CSL method is potentially a better, more natural choice for solutions of the fully-compressible, non-hydrostatic equations — the CSL method better preserves the mathematical and physical properties of these systems.

The extension to the multi-dimensional problems is also discussed and a simple demonstration is presented. In addition to this work, we are also developing a general minimization algorithm that treats both decoupling and solution procedures simultaneously, and we will apply it to the general testing problems of non-hydrostatic atmospheric models, such as flow over mountains or density currents.

ACKNOWLEDGMENTS

This work was supported by the National Science Foundation under grant No. EAR0196048 with the University of Central Florida.

REFERENCES

Bannon, P. R., 1995: Hydrostatic adjustment: Lamb's problem, *J. Atmos. Sci.*, **52**, 1743–1752.

Courant, R., and D. Hilbert, 1962: *Methods of Mathematical Physics*, Volume II. Interscience Publishers, 830 pp.

Deconinck, H., C. Hirsch, and J. Peuteman, 1986: Characteristic decomposition methods for the multi-dimensional Euler equations, The 10th International Conference on Numerical Methods in Fluid Dynamics, Beijing, China.

Durran, D. R., 1999: Numerical Methods for Wave Equations in Geophysical Fluid Dynamics, *Texts in Applied Mathematics*, 32. New York, Springer. 465pp.

Durran, D. R., 2001: Open boundary conditions: Fact and fiction, *IUTAM Symposium on Advances in Mathematical Modeling of Atmosphere and Ocean Dynamics*, P. F. Hodnett, Ed., Kluwer Academic Publishers, pp. 1–18.

Erbes, G., 1993: A semi-Lagrangian method of characteristics for the shallow-water equations. *Mon. Wea. Rev.*, **121**, 3443–3452.

Gill, A. E., 1982: *Atmosphere-Ocean Dynamics*, Academic Press. 662pp.

Gustafsson, B., H.-O. Kress, and J. Oliger, 1995: *Time Dependent Problems and Difference Methods*, John Wiley & Sons, 642pp.

Hirsch, C., 1988: *Numerical Computation of Internal and External Flows, Volume 1: Fundamentals of Numerical Discretization*, John Wiley & Sons, 515pp.

Hirsch, C., 1990: *Numerical Computation of Internal and External Flows, Volume 2: Computational Methods for Inviscid and Viscous Flows*, John Wiley & Sons, 691pp.

Kulikovskii, A. G., N. V. Pogorelov, and A. Y. Semenov, 2001: Mathematical Aspects of Numerical Solutions of Hyperbolic Systems, *Chapman & Hall/CRC Monographs and Surveys in Pure and Applied Mathematics*, **118**, 54pp.

Kuo, A. C., and L. M. Povani, 1997: Time-dependent fully nonlinear geostrophic adjustment, *J. Phys. Oceanogr.*, **27**, 1614–1634.

Lax, P. D., 1973: Hyperbolic systems of conservation laws and the mathematical theory of shock waves, *CBMS-NSF Regional Conference Series in Applied Mathematics*, No.11.

Poinsot, T. J., and S. K. Lele, 1992: Boundary conditions for direct simulations of compressible viscous flows, *J. Comput. Phys.*, **101**, 104–129.

Sotack, T., and P. R. Bannon, 1999: Lamb's hydrostatic adjustment for heating of finite duration, *J. Atmos. Sci.*, **56**, 71–81.

Staniforth, A. and J. Cote, 1991: Semi-Lagrangian integration schemes for atmospheric models—A review, *Mon. Wea. Rev.*, **114**, 2206–2223.

Tanguay, M. A., A. Robert, and R. Laprise, 1990: A semi-implicit semi-Lagrangian fully compressible regional forecast model, *Mon. Wea. Rev.*, **118**, 1970–1980.

Toro, E. F., 2001: *Shock-Capturing Methods for Free-Surface Shallow Flows*, Chichester [England]; New York; John Wiley, 309pp.

Williamson, D. L., and P. J. Rasch, 1989: Two-dimensional semi-Lagrangian transport with shape-preserving interpolation, *Mon. Wea. Rev.*, **117**, 102–129.

APPENDIX

A Semi-Implicit, Semi-Lagrangian Method for a 1-D Non-hydrostatic Atmospheric Model

For comparison with the CSL method, a semi-implicit, semi-Lagrangian (SISL) method is developed for the 1-D non-hydrostatic atmospheric model. It is a two-time-level scheme. Otherwise, it is similar to the SISL method used in the MC2 model (Tanguay et al., 1990).

The 1-D non-hydrostatic atmospheric equations can be written as

$$\frac{\partial \rho}{\partial t} + w\frac{\partial w}{\partial z} + \rho\frac{\partial w}{\partial z} = 0, \tag{A1}$$

$$\frac{\partial w}{\partial t} + w\frac{\partial w}{\partial z} + \frac{\gamma R\pi}{\rho}\frac{\partial \Theta}{\partial z} = -g, \tag{A2}$$

$$\frac{\partial \Theta}{\partial t} + w\frac{\partial \Theta}{\partial z} + \Theta\frac{\partial w}{\partial z} = \rho\dot{Q}. \tag{A3}$$

The notation is standard. Define

$$\frac{DF}{Dt} = \frac{\partial F}{\partial t} + w\frac{\partial F}{\partial z},$$

and a hydrostatic reference state $(\bar{\rho}, \bar{\Theta})$, such that $\rho' = \rho - \bar{\rho}, \Theta' = \Theta - \bar{\Theta}$. The 1-D non-hydrostatic atmospheric model equations can then be written as

$$\frac{D\rho'}{Dt} + w\frac{\partial \bar{\rho}}{\partial z} + \bar{\rho}\frac{\partial w}{\partial z} = R_\rho, \tag{A4}$$

$$\frac{Dw}{Dt} + \frac{\gamma R\bar{\pi}}{\bar{\rho}}\frac{\partial \Theta'}{\partial z} + g(\frac{\rho'}{\bar{\rho}} - \frac{R}{c_v}\frac{\Theta'}{\bar{\Theta}}) = R_w, \tag{A5}$$

$$\frac{D\Theta'}{Dt} + w\frac{\partial \bar{\Theta}}{\partial z} + \bar{\Theta}\frac{\partial w}{\partial z} = R_\Theta, \tag{A6}$$

where

$$R_\rho = -\rho'\frac{\partial w}{\partial z}, \tag{A7}$$

$$R_w = -\gamma R(\frac{\pi}{\rho} - \frac{\bar{\pi}}{\bar{\rho}})\frac{\partial \Theta'}{\partial z} + g(\frac{\bar{\rho}}{\rho}\frac{\pi'}{\bar{\pi}} - \frac{R}{c_v}\frac{\Theta'}{\bar{\Theta}}) + \frac{g\rho'^2}{\bar{\rho}\rho}, \tag{A8}$$

$$R_\Theta = -\Theta'\frac{\partial w}{\partial z} + \rho\dot{Q}. \tag{A9}$$

Define the Lagrangian time-difference, time-average, and trajectory-average operators as

$$\frac{D\psi}{Dt} = \frac{\psi(z,t) - \psi(z-\lambda, t-\Delta t)}{\Delta t}, \tag{A10}$$

$$\overline{\psi}^{\mathrm{t}} = [(1+\epsilon)\psi(z,t) + (1-\epsilon)\psi(z-\lambda, t-\Delta t)]/2, \tag{A11}$$

$$\overline{R}_\psi^{\mathrm{traj}} = [R_\psi(z,t) + R_\psi(z-\lambda, t)]/2, \tag{A12}$$

and the Lagrangian displacement as

$$\lambda = \Delta t[w(z,t) + w(z-\lambda, t-\Delta t)]/2. \tag{A13}$$

Applying (A10) to the first of, and (A11) to the rest of, the left-hand side terms of Eqs. (A5)–(A6); and (A12) to the right-hand side of Eqs. (A5)–(A6), we can then obtain the two-time-level SISL equations of the following form:

$$Q_\psi(z,t) = P_\psi(z-\lambda, t-\Delta t) + \Delta t\overline{R}_\psi^{\mathrm{traj}}, \tag{A14}$$

where, for the Q_ψ terms at time t, we have

$$\rho' + \frac{1}{2}(1+\epsilon)\Delta t(\bar{\rho}\frac{\partial w}{\partial z} + w\frac{\partial \bar{\rho}}{\partial z}) = Q_\rho, \tag{A15}$$

$$w + \frac{1}{2}(1+\epsilon)\Delta t(\frac{\gamma R\bar{\pi}}{\bar{\rho}} + g\frac{\rho'}{\bar{\rho}} - g\frac{R}{c_v}\frac{\Theta'}{\bar{\Theta}}) = Q_w, \tag{A16}$$

$$\Theta' + \frac{1}{2}(1+\epsilon)\Delta t(\bar{\Theta}\frac{\partial w}{\partial z} + w\frac{\partial \bar{\Theta}}{\partial z}) = Q_\Theta, \tag{A17}$$

and the P_ψ terms at time $(t - \Delta t)$ are

$$P_\rho = \rho' - \frac{1}{2}(1-\epsilon)\Delta t(\bar{\rho}\frac{\partial w}{\partial z} + w\frac{\partial \bar{\rho}}{\partial z}), \tag{A18}$$

$$P_w = w - \frac{1}{2}(1-\epsilon)\Delta t(\frac{\gamma R\bar{\pi}}{\bar{\rho}} + g\frac{\rho'}{\bar{\rho}} - g\frac{R}{c_v}\frac{\Theta'}{\bar{\Theta}}), \tag{A19}$$

$$P_\Theta = \Theta' - \frac{1}{2}(1-\epsilon)\Delta t(\bar{\Theta}\frac{\partial w}{\partial z} + w\frac{\partial \bar{\Theta}}{\partial z}), \tag{A20}$$

and the R_ψ are given by (A7)–(A9). Eliminating ρ' and Θ' from (A15)–(A17), we obtain an equation for w at time t in the following form:

$$C_1\frac{\partial^2 w}{\partial z^2} + C_2\frac{\partial w}{\partial z} + w = A_1, \tag{A21}$$

where

$$C_1 = -[\frac{1}{2}(1+\epsilon)\Delta t]^2 \bar{c}^2,$$
$$C_2 = +[\frac{1}{2}(1+\epsilon)\Delta t]^2 g \frac{c_p}{c_v},$$
$$A_1 = Q_w - \frac{1}{2}(1+\epsilon)\Delta t(\frac{\bar{c}^2}{\bar{\Theta}}\frac{\partial Q_\Theta}{\partial z} + g\frac{Q_\rho}{\bar{\rho}} - g\frac{R}{c_v}\frac{Q_\Theta}{\bar{\Theta}}).$$

Discretization of (A21) gives a linear equation system with a tridiagonal matrix, which can be easily solved to obtain w. Once we have w, we can solve (A15) and (A17) for ρ' and Θ', respectively.